

Identification of Dysregulated Pathways Associated with Ankylosing Spondylitis Using Pathway Interaction Network

Zhi-Hua Wang,¹ Dong Xiang,¹ Jun-Jie Dong,² Shao-Xuan He,¹ Li-Min Guo,¹ Jia Lv,¹ Wei Wei,¹ Nan-Nan Kou,¹ and Jun Shu^{3,*}

¹Department of Traumatology, The Second Affiliated Hospital of Kunming Medical University, Kunming, 650011, Yunnan Province, China

²Department of Orthopedics, First Affiliated Hospital of Kunming Medical University, Kunming, 650032, Yunnan Province, China

³Department of Orthopedics, The Second Affiliated Hospital of Kunming Medical University, Kunming, 650011, Yunnan Province, China

*Corresponding author: Jun Shu, Department of Orthopedics, The Second Affiliated Hospital of Kunming Medical University, No.374 on Kunrui Road, Wuhua District, Kunming, 650011, Yunnan Province, China. Tel: +86-087165351157, Fax: +86-087165351157, E-mail: junshukunming@yeah.net

Received 2016 November 10; Revised 2017 February 20; Accepted 2017 March 25.

Abstract

Background: Pathway analysis is the first choice for gaining insight into the underlying biology of disease, as it reduces complexity and increases explanatory power.

Objectives: The purpose of our paper was to investigate dysregulated pathways between ankylosing spondylitis (AS) patients as well as normal controls based on the pathway interaction network (PIN) related analysis.

Methods: This is a case-control bioinformatics analysis using already published microarray data of AS. It was conducted in Kunming, China from October 2015 to June 2016. We recruited the gene expression profile of AS from the ArrayExpress database (<http://www.ebi.ac.uk/arrayexpress/>) with the accessing number of E-GEOD-25101. E-GEOD-25101 existed on A-MEXP-1171 - Illumina HumanHT-12 v3.0 Expression BeadChip Platform and was comprised of 32 samples (16 AS samples and 16 normal samples). Meanwhile, the protein-protein interaction (PPI) data and pathway data were retrieved from Search Tool for the retrieval of interacting genes/proteins (STRING, <http://string-db.org/>) as well as Reactome databases, respectively. Furthermore, according to the principal component analysis (PCA) method, the seed pathway was selected by computing the activity score for each pathway. A PIN was constructed dependent on the data and Pearson correlation coefficient (PCC). Dysregulated pathways were captured from the PIN by utilizing the seed pathway and the area under the receiver operating characteristics curve (AUROC) index.

Results: The PIN consisted of 1022 pathways and 7314 interactions, of which, 3'-UTR-mediated translational regulation was the seed pathway (absolute change of activity score = 10.962). Starting from the seed pathway, a minimum set of pathways with AUROC = 0.902 was extracted from the PIN. Consequently, a total of 11 dysregulated pathways were identified for AS compared with normal controls, such as L13a-mediated translational silencing of Ceruloplasmin expression, GTP hydrolysis, as well as joining of the 60S ribosomal subunit.

Conclusions: These results might be available to provide potential biomarkers to diagnose AS as well as give a hand to reveal pathological mechanism of this disease.

Keywords: Ankylosing, Spondylitis, Pathway, Interaction, Network

1. Background

Ankylosing spondylitis (AS), an immune-mediated arthritis, is the prototypic member of a group of conditions known as spondyloarthropathies, which also includes reactive arthritis, psoriatic arthritis, and enteropathic arthritis (1). Several features such as synovitis, chondroid metaplasia, cartilage destruction, and subchondral bone marrow changes are commonly found in the joints of AS patients (2). Due to the complex progression of the joint remodeling process, clinical researches do not systematically evaluate histopathologic changes (3) and no clear sequence of the pathological mechanism can yet be drawn from AS. Therefore, it is understandable that major efforts

have been done for dissecting the potential mechanisms underlying AS.

With the advances of high-throughput technologies, it has been widely applied to explore diagnostic signatures, provide novel insights into the underlying molecular mechanisms, and shed new lights on the aetiopathogenesis of human diseases (4). Currently, rapid progress has been made in discovering genetic associations with AS (5-7). For instance, it had been reported that approximately 90% of AS patients expressed the major histocompatibility complex, class I, B27 (HLA-B27) (6). Furthermore, Lin et al. (7) investigated the pathophysiological significance of Interleukin (IL)-27 and vascular endothelial growth factor (VEGF) in AS. However, the exact mechanism of AS is still

unclear and is needed to urgently be disclosed and uncovered.

Generally speaking, genes are not only encoded as individual genes or proteins, but also interacted with others to form interactions (8). Moreover, approximate genes and interactions may play similar functions and are enriched in a biological pathway (9). Pathway analysis has become the first choice for gaining insight into the underlying biology of genes and proteins, as it reduces complexity and has increased explanatory power (10). Altered pathways give insights to the molecular targets and therefore, researchers have paid more attention to this concept. For example, Wnt pathway was revealed to play a critical contributing role in the unique pathology and bony fusion in AS (11). Considering the complicated nature of biological systems, more than 1 pathway might be involved in a given complex disease and the deregulation of 1 pathway may affect the activities of many related pathways (12). It is possible to detect more reliable pathway biomarkers by taking into account the functional dependency or interaction between pathways, that is to say, the pathway interaction network (PIN).

Therefore, in the current study, we constructed a PIN and utilized it to identify dysregulated pathways between AS patients and normal controls. Specifically, after the genes were aligned to the pathways, we utilized the principal component analysis (PCA) method to compute the pathway activity for each pathway relying on the summary of the expression values of all genes in this given pathway, and selected the seed pathway. After, the PIN was constructed with each node representing a biological pathway based on gene expression data, protein-protein interactions (PPIs) data, and pathway data. Eventually, dysregulated pathways were extracted from the PIN utilizing seed pathway and the area under the receiver operating characteristics curve (AUROC) index.

2. Methods

2.1. Preparing Datasets

2.1.1. Gene Expression Data

This study is a case-control bioinformatics analysis using already published microarray data of ankylosing spondylitis. A gene expression dataset of AS with the accession number E-GEOD-25101 was collected from the ArrayExpress database (<http://www.ebi.ac.uk/arrayexpress/>). E-GEOD-25101 existed on A-MEXP-1171 - Illumina HumanHT-12 v3.0 Expression BeadChip Platform and was comprised of 32 samples (16 ankylosing spondylitis samples and 16 normal samples). For the purpose of improving the quality of the data, standard pre-treatments were conducted,

including robust multi-array average (RMA) algorithm for background correction (13), quantiles algorithm for normalization (14), micro array suite (MAS) algorithm to revise the perfect match and mismatch (15), and median-polish method for summarization of all expression values (13). Based on the preprocessed data on the probe level, we mapped them into a gene symbol measure, a total of 11587 genes were obtained in the gene expression data for further exploitation.

2.1.2. PPI Data

The human PPIs on 16730 protein entries and 787896 interactions was retrieved from the search tool for the retrieval of interacting genes/proteins (STRING) database (16), which provides a critical assessment and integration of PPIs, including direct (physical) as well as indirect (functional) associations, and is widely used in various studies (17). Subsequently, in order to make these PPIs more reliable and correlated to AS, we discarded interactions with a score < 0.2. Note that the score was the inherent score of an interaction in the STRING database. Furthermore, the reserved interactions were integrated with the gene expression data to take their intersections. Ultimately, 266199 interactions among 9865 genes were retained and termed with PPI data for the present study.

2.1.3. Pathway Data

All biological pathways for human beings (1675 pathways) were captured from a confirmed Reactome pathway database, which is a manually curated open-source open-data resource of human pathways and provides infrastructure for computation across the biologic reaction network (18). As the same with PPI data, we also took intersections between the 1675 pathways and gene expression data. In addition, pathways with very few genes might not have sufficient biological information and too many genes may be too generic (19), thus, only pathways of intersected gene amounts ranged from 5 to 100 were reserved as our study objectives. Finally, we obtained 1022 pathways and assigned an ID to each pathway in accordance with its alphabetical order.

2.2. Computing Pathway Activity

To further explore biological functions and importance for pathways in pathway data, an activity score for each pathway was defined as the summary of the expression levels of all genes enriched in this given pathway utilizing the PCA method (20). The PCA technique can effectively characterize the internal structure of the high-dimension dataset by preserving the variance in the data while transforming the data into low-dimension space (12).

In short, the activity score of pathway k in sample j , P_{kj} , was a linear combination of the expressions of all genes in the pathway:

$$P_{kj} = w_{1jk}x_{1jk} + w_{2jk}x_{2jk} \cdots + w_{ijk}x_{ijk} \quad (1)$$

Where x_{ijk} stood for the standardized expression value of gene i from pathway k in sample j , and w_{ijk} denoted weight of x_{ijk} . Particularly, the first principal component from PCA was defined as the activity score for the corresponding pathway. Note that the activity score for 1 pathway across disease and normal controls was different and the difference might indicate its correlation to the disease, the bigger of the difference, and the closer relevance of this pathway to the disease. Thus, in the current study, the pathway with a maximum change of activity score between disease and control groups was defined as seed pathway.

2.3. Constructing PIN

In the present work, a PIN was constructed with each node standing for a pathway, where 1 edge was laid between 2 pathways if they shared at least 1 gene or there were interactions between genes from the 2 pathways based on the PPI data. In other words, edges in PIN must satisfy at least 1 of 2 conditions. The first condition requested that at least 1 of the common genes between 2 pathways is differentially expressed between AS patients and normal controls. Student's t-test was applied to perform differentially expression analyses for genes, which determines whether 2 populations express a significant or non-significant difference between population means (21). Only the genes that met to the threshold of $P < 0.05$ were regarded as differentially expressed between AS status and normal controls.

The other condition required that the 2 genes that coded a pair of interacting genes used to lay an edge between 2 pathways were highly co-expressed (absolute value of $PCC > 0.8$). Importantly, PCC is one of the commonly used measures for the strength of the association between a pair of variables, giving a value between -1 and +1 inclusive (22). We computed the PCC for all interactions in PPI data, thereby gaining the distribution of PCC and also calculated the absolute difference of PCC across AS samples and normal controls. If the edge between 2 pathways met to 1 of the 2 conditions, it would be reserved or else discarded. Meanwhile, it had been reported that a excessively big network might neglect a certain number of significant genes and interactions (23), thus we selected the top 5% pathways, in descending order, of absolute value of PCC to construct the PIN for AS.

2.4. Identifying Dysregulated Pathways

After computing the activity score for each pathway and defining the seed pathway, we formulated the identification of dysregulated pathways as a feature selection problem in a machine learning framework, where the minimum set of pathways that can best discriminate diseases from controls were considered to be more possibly dysregulated pathways. In the feature selection, the support vector machines (SVMs) model was utilized, which is a widely used kernel based method especially useful for a small number of samples with high dimensional variables (24). Concretely, starting with the seed pathway, the minimum set of pathways search step iteratively involved pathways whose addition led to the maximum increase in the prediction accuracy pathway set until the prediction accuracy dropped. The prediction accuracy capability or classification performance was evaluated by AUROC index (25), and the performance ability was tested using five-fold cross validation (26). In the five-fold cross validation, all samples were randomly divided into 5 equal-size parts, 4 of which were employed as training set but the others were used as test set to evaluate the classification performance. In order to get robust results and ensure accuracy of classified performance, we repeated computing AUROC 100 times when adding a new pathway and the average was used as the final result.

3. Results

3.1. PIN

In this work, 3 kinds of data were collected, gene expression data of 11587 genes, PPI data with 9865 genes and 266199 interactions, as well as a pathway data of 1022 pathways. Using the gene expression data, 2280 genes were detected to be differentially expressed between AS patients and normal control based on the Student's t-test. When an interaction between 2 pathways satisfied that at least 1 of the common genes of the 2 pathways was differentially expressed, or the 2 pathways were highly co-expressed (absolute difference of $PCC > 0.8$), it would be retained or else removed. In consequence, 146286 interactions were gained. With the purpose of reducing the intricate network, we adopted the top 5% of all interaction to construct a PIN. The PIN was comprised of 7314 interactions and 1022 nodes, in which we defined the absolute value of PCC for an edge as its score. Interestingly, we found that 11 pathway interactions had the score values higher than 400, as displayed in Table 1. A total of 10 pathways participated in the 11 interactions, of which DNA replication (ID: 234) and synthesis of DNA (ID: 890) appeared 5 times. Besides, the interaction between mRNA Splicing (ID: 511) and mRNA Splicing - Major Pathway (ID: 512) possessed the largest score of 456914.

Table 1. Interactions with Score > 400 in Pathway Interaction Network (PIN)^a

Rank	Interaction		Score
	Pathway (ID)	Pathway (ID)	
1	511	512	456.914
2	59	234	445.106
3	234	722	445.105
4	234	890	431.017
5	59	890	418.592
6	722	890	418.590
7	234	235	409.995
8	234	464	409.945
9	235	890	409.066
10	464	890	409.065
11	366	869	403.474

^aThe pathway name for ID: 511, mRNA Splicing; 512, mRNA Splicing - Major Pathway; 59, APC/C-mediated degradation of cell cycle proteins; 234, DNA Replication; 722, Regulation of mitotic cell cycle; 890, Synthesis of DNA; 235, DNA Replication Pre-Initiation; 464, M/G1 Transition; 366, GTP hydrolysis and joining of the 60S ribosomal subunit; 869, SRP-dependent cotranslational protein targeting to membrane.

3.2. Seed Pathway

To investigate the significances for pathways in pathway data, an activity score was assigned to each pathway according to the PCA method. As described above, we uncovered that the activity score for certain pathway in AS patients was different from that of normal controls. Furthermore, how to overcome the inconsistent results and set standards to assess the importance of pathways had become a great challenge. After careful thinking, the absolute change of activity score across AS and normal samples was denoted as the activity score for the pathway. The distribution for absolute activity score changes for 1022 pathways was illustrated in Figure 1. With the increase of the absolute change value, the number of pathways decreased, especially after 5829. Of note, we found that significant change of the activity score between AS and normal groups happened in the pathway of 3'-UTR-mediated translational regulation (Absolute change of activity score = 10.962), which thus defined this pathway as seed pathway.

3.3. Dysregulated Pathways

As mentioned above, 3'-UTR-mediated translational regulation (ID: 1) was the seed pathway. Beginning with this seed pathway, selection of dysregulated pathways was implemented according to the classification accuracy. This procedure stopped until classification accuracy was not increased. Ultimately, a minimum set (AUROC = 0.902) of

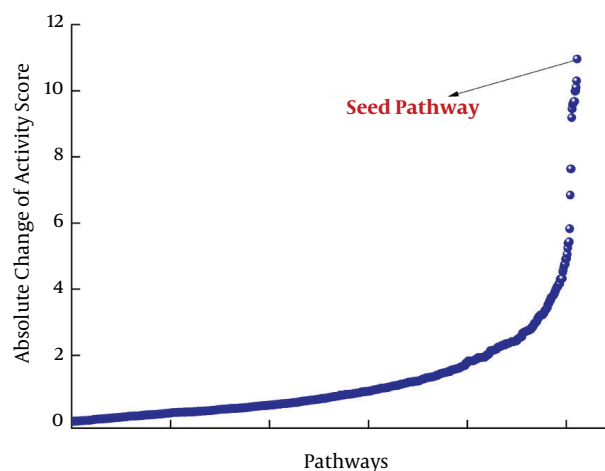


Figure 1. Distributions of absolute activity score changes for pathways in pathway data. The pathway of activity score with the greatest change between ankylosing spondylitis (AS) patients and normal controls was considered to be seed pathway.

pathways was extracted from the PIN (Figure 1), which indicated that these selected dysregulated pathways could be utilized as robust bio-signatures. As shown in Figure 2, there were 11 dysregulated pathways that interacted with 44 interactions, in which the red node represented the seed pathway 3'-UTR-mediated translational regulation.

4. Discussion

In this paper, we extracted the dysregulated pathways, which were able to distinguish AS patients from normal controls, dependent on the PIN related analysis. Consequently, a PIN with 1022 nodes and 7314 interactions were gained for the AS group. Subsequently, the seed pathway was defined as the highest absolute change of activity score between AS patients and normal controls though the PCA method. Furthermore, a minimum set of pathways with 11 nodes and 44 interactions was extracted from the PIN. As mentioned above, pathways in this set were dysregulated pathways. It was reasonable and biologically interpretable to denote these pathways in the set as discriminative features between AS samples and normal controls. A seed pathway that can best discriminate between the experimental group and control was firstly identified as the first pathway biomarker. The second pathway that can be combined with the first pathway to get better classification results was identified from those pathways that interacted with the first pathway in PIN (12).

In particular, 3'-UTR-mediated translational regulation was the seed pathway. With our knowledge, the specific interaction of factor (s) with the 5' or 3' untranslated region

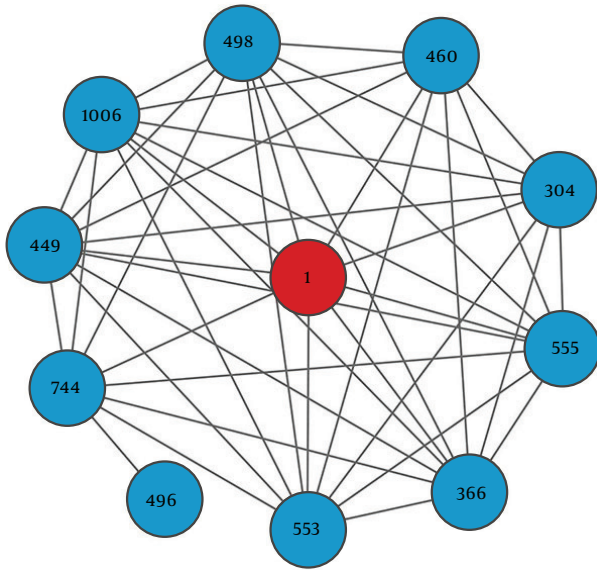


Figure 2. Interaction network of dysregulated pathways. Nodes represented pathways, and edges were the interaction among any two pathways. The red node was the seed pathway. The ID verse dysregulated pathway, 1: 3'-UTR-mediated translational regulation; 449: L13a-mediated translational silencing of Ceruloplasmin expression; 366: GTP hydrolysis and joining of the 60S ribosomal subunit; 553: nonsense mediated decay (NMD) enhanced by the exon junction complex (EJC); 555: nonsense-mediated decay (NMD); 1006: viral mRNA translation; 744: respiratory electron transport, ATP synthesis by chemiosmotic coupling, and heat production by uncoupling proteins; 960: translation initiation complex formation; 498: mitochondrial translation elongation; 304: formation of the ternary complex, and subsequently, the 43S complex; and 496: mitochondrial protein import.

(UTR) drove transcript-selective and translational control, thereby influencing initiation, elongation, or termination of mRNA translation (27). Besides, translational control provides numerous advantages in regulation of gene expression including rapid responsiveness, intracellular localization, and coordinated regulation of transcript ensembles (28, 29). New and unexpected mechanisms of 3'-UTR-mediated translational regulation as well as their contributions to the disease have received increasing attention during the last decade, emphasizing the novel aspects of these regulatory mechanisms and their potential pathophysiological significance (30). Hence, we knew that 3'-UTR-mediated translational regulation took active participated in various biological processes no matter in normal or disease samples, and inferred that the dysregulation of this pathway might be one of the possible leading causes. It is the first time to uncover the relationship between 3'-UTR-mediated translational regulation and AS patients.

When bringing inhibitory 3'-UTR-binding proteins into a position in which they interfere with either the function of the translation initiation complex or with the assembly of the ribosome, the circularization of mRNA during translation initiation contributes an increase in the effi-

ciency of translation and appears to provide a mechanism for translational silencing (31). Translational silencing is mediated by the L13a subunit and thought to require circularization of the Ceruloplasmin (Cp) mRNA (32). Moreover, phosphorylated L13a associates with the GAIT element in the 3' UTR of the Cp mRNA inhibiting its translation. Thus L13a-mediated translational silencing of Ceruloplasmin expression co-operated with the seed pathway closely, which validated that the feasibility of the dysregulated pathway set.

Meanwhile, there were several limitations in this work. The samples utilized for obtaining the microarray data were retrieved from the public database, not from our own department. Moreover, the work was a pure bioinformatics analysis and the results were not verified by wet experiments. In the paper, we have identified 11 dysregulated pathways between AS patients and normal controls based on the PIN correlated analyses. The results suggested dysregulated pathways, especially 3'-UTR-mediated translational regulation, were important to the progression of AS development. Furthermore, they also gave great insights to reveal the pathological mechanism underlying this disease. However, the validation of these dysregulated pathways should be conducted as soon as possible.

Acknowledgments

This research received no specific grants from any funding agency in public, commercial, or not-for-profit sectors.

Footnote

Conflict of Interests: We state that there is no conflict of interests in this paper.

References

1. Fellow JCW, Liu C. Sulfasalazine for ankylosing spondylitis. *Cochrane Database Systematic Reviews*. 2014;**11**(2).
2. Bleil J, Maier R, Hempfing A, Schlichting U, Appel H, Sieper J, et al. Histomorphologic and histomorphometric characteristics of zygapophyseal joint remodeling in ankylosing spondylitis. *Arthritis Rheumatol*. 2014;**66**(7):1745-54. doi: [10.1002/art.38404](https://doi.org/10.1002/art.38404). [PubMed: [24574301](https://pubmed.ncbi.nlm.nih.gov/24574301/)].
3. Mark S, Helen D, Karl G. Comment on: 'Diagnostic delay in patients with rheumatoid arthritis, psoriatic arthritis and ankylosing spondylitis: results from the Danish nationwide DANBIO registry' by S? *Cerebrovascular Diseases*. 2015;**73**(7):44.
4. Jordan F, Nguyen TP, Liu WC. Studying protein-protein interaction networks: a systems view on diseases. *Brief Funct Genomics*. 2012;**11**(6):497-504. doi: [10.1093/bfpg/els035](https://doi.org/10.1093/bfpg/els035). [PubMed: [22908210](https://pubmed.ncbi.nlm.nih.gov/22908210/)].
5. Brown MA, Kenna T, Wordsworth BP. Genetics of ankylosing spondylitis-insights into pathogenesis. *Nat Rev Rheumatol*. 2016;**12**(2):81-91. doi: [10.1038/nrrheum.2015.133](https://doi.org/10.1038/nrrheum.2015.133). [PubMed: [26439405](https://pubmed.ncbi.nlm.nih.gov/26439405/)].

6. Colbert RA, Tran TM, Layh-Schmitt G. HLA-B27 misfolding and ankylosing spondylitis. *Mol Immunol.* 2014;57(1):44–51. doi: [10.1016/j.molimm.2013.07.013](https://doi.org/10.1016/j.molimm.2013.07.013). [PubMed: 23993278].
7. Lin TT, Lu J, Qi CY, Yuan L, Li XL, Xia LP, et al. Elevated serum level of IL-27 and VEGF in patients with ankylosing spondylitis and associate with disease activity. *Clin Exp Med.* 2015;15(2):227–31. doi: [10.1007/s10238-014-0281-x](https://doi.org/10.1007/s10238-014-0281-x). [PubMed: 24710630].
8. Vinayagam A, Zirin J, Roesel C, Hu Y, Yilmazel B, Samsonova AA, et al. Integrating protein-protein interaction networks with phenotypes reveals signs of interactions. *Nat Methods.* 2014;11(1):94–9. doi: [10.1038/nmeth.2733](https://doi.org/10.1038/nmeth.2733). [PubMed: 24240319].
9. Jin D, Lee H. A computational approach to identifying gene-microRNA modules in cancer. *PLoS Comput Biol.* 2015;11(1):e1004042. doi: [10.1371/journal.pcbi.1004042](https://doi.org/10.1371/journal.pcbi.1004042). [PubMed: 25611546].
10. Glazko GV, Emmert-Streib F. Unite and conquer: univariate and multivariate approaches for finding differentially expressed gene sets. *Bioinformatics.* 2009;25(18):2348–54. doi: [10.1093/bioinformatics/btp406](https://doi.org/10.1093/bioinformatics/btp406). [PubMed: 19574285].
11. Corr M. Wnt signaling in ankylosing spondylitis. *Clin Rheumatol.* 2014;33(6):759–62. doi: [10.1007/s10067-014-2663-6](https://doi.org/10.1007/s10067-014-2663-6). [PubMed: 24820146].
12. Liu KQ, Liu ZP, Hao JK, Chen L, Zhao XM. Identifying dysregulated pathways in cancers from pathway interaction networks. *BMC Bioinformatics.* 2012;13:126. doi: [10.1186/1471-2105-13-126](https://doi.org/10.1186/1471-2105-13-126). [PubMed: 22676414].
13. Irizarry RA, Bolstad BM, Collin F, Cope LM, Hobbs B, Speed TP. Summaries of Affymetrix GeneChip probe level data. *Nucleic Acids Res.* 2003;31(4):e15. [PubMed: 12582260].
14. Bolstad BM, Irizarry RA, Astrand M, Speed TP. A comparison of normalization methods for high density oligonucleotide array data based on variance and bias. *Bioinformatics.* 2003;19(2):185–93. [PubMed: 12538238].
15. Bolstad BA. Built-in processing methods. 2013
16. Szklarczyk D, Franceschini A, Kuhn M, Simonovic M, Roth A, Minguéz P, et al. The STRING database in 2011: functional interaction networks of proteins, globally integrated and scored. *Nucleic Acids Res.* 2011;39(Database issue):D561–8. doi: [10.1093/nar/gkq973](https://doi.org/10.1093/nar/gkq973). [PubMed: 21045058].
17. Szklarczyk D, Franceschini A, Wyder S, Forslund K, Heller D, Huerta-Cepas J, et al. STRING v10: protein-protein interaction networks, integrated over the tree of life. *Nucleic Acids Res.* 2015;43(Database issue):D447–52. doi: [10.1093/nar/gku1003](https://doi.org/10.1093/nar/gku1003). [PubMed: 25352553].
18. Croft D, Mundo AF, Haw R, Milacic M, Weiser J, Wu G, et al. The Reactome pathway knowledgebase. *Nucleic Acids Res.* 2014;42(Database issue):D472–7. doi: [10.1093/nar/gkt1102](https://doi.org/10.1093/nar/gkt1102). [PubMed: 24243840].
19. Ahn T, Lee E, Huh N, Park T. Personalized identification of altered pathways in cancer using accumulated normal tissue data. *Bioinformatics.* 2014;30(17):i422–9. doi: [10.1093/bioinformatics/btu449](https://doi.org/10.1093/bioinformatics/btu449). [PubMed: 25161229].
20. Bro R, Smilde AK. Principal component analysis. *Analytical Method.* 2014;6(9):2812–31.
21. Haynes W. Student's t-test. *Encyclopedia of systems biology.* Springer; 2013. pp. 2023–5.
22. Nahler G. Pearson correlation coefficient. *Dictionary of Pharmaceutical Medicine;* 2009. p. 132.
23. Nibbe RK, Chowdhury SA, Koyuturk M, Ewing R, Chance MR. Protein-protein interaction networks and subnetworks in the biology of disease. *Wiley Interdiscip Rev Syst Biol Med.* 2011;3(3):357–67. doi: [10.1002/wsbm.121](https://doi.org/10.1002/wsbm.121). [PubMed: 20865778].
24. Chang CC, Lin CJ. Libsvm. *ACM Transaction Intel System Technol.* 2011;2(3):1–27. doi: [10.1145/1961189.1961199](https://doi.org/10.1145/1961189.1961199).
25. Huang J, Ling CX. Using AUC and accuracy in evaluating learning algorithms. *Knowledge Data Engin.* 2005;17(3):299–310.
26. Rojatk DV, Chinchkhede KD, Sarate GG. Handwritten Devnagari consonants recognition using MLPNN with five fold cross validation. *International Conference on Circuits, Power and Computing Technologies;* 2013.
27. Medenbach J, Seiler M, Hentze MW. Translational control via protein-regulated upstream open reading frames. *Cell.* 2011;145(6):902–13. doi: [10.1016/j.cell.2011.05.005](https://doi.org/10.1016/j.cell.2011.05.005). [PubMed: 21663794].
28. Hadziselimovic N, Vukojevic V, Peter F, Milnik A, Fastenrath M, Fenyves BG, et al. Forgetting is regulated via Musashi-mediated translational control of the Arp2/3 complex. *Cell.* 2014;156(6):1153–66. doi: [10.1016/j.cell.2014.01.054](https://doi.org/10.1016/j.cell.2014.01.054). [PubMed: 24630719].
29. Mazumder B, Seshadri V, Fox PL. Translational control by the 3'-UTR: the ends specify the means. *Trends Biochem Sci.* 2003;28(2):91–8. doi: [10.1016/S0968-0004\(03\)00002-1](https://doi.org/10.1016/S0968-0004(03)00002-1). [PubMed: 12575997].
30. Jia J, Yao P, Arif A, Fox PL. Regulation and dysregulation of 3'UTR-mediated translational control. *Curr Opin Genet Dev.* 2013;23(1):29–34. doi: [10.1016/j.gde.2012.12.004](https://doi.org/10.1016/j.gde.2012.12.004). [PubMed: 23312843].
31. Mrugasiewicz M. Monte carlo study of phonon transport in solid thin films including dispersion and polarization. *J Heat Transfer.* 2001;123(4):749–59.
32. Mazumder B, Sampath P, Seshadri V, Maitra RK, DiCorleto PE, Fox PL. Regulated release of L13a from the 60S ribosomal subunit as a mechanism of transcript-specific translational control. *Cell.* 2003;115(2):187–98. [PubMed: 14567916].